論 文
40～12～4

유도전동기 서보운전을 위한 마이크로프로세서-벡터 제어 시스템

Microprocessor-Based Vector Control System for Induction Motor Servo-Drive

金 垙 憲* · 金 暎 烈* · 元 忠 淵** · 元 鍾 洙***
(Gwang-Heon Kim · Young-Real Kim · Chung-Yuen Won · Jong-Soo Won)

Astract - The time optimal position control design can be repeatedly taken from the initial state of a dynamic system to a desired one as fast as possible in the industrial drives. In this case, an induction machine parameters will vary due to temperature, frequency, and saturation effects. In particular, the rotor resistance changes critically with temperature and frequency. These changes affect the command values of the stator current components and slip speed. There is a mismatch between the commanded variables and actual ones of the induction motor drive, and this situation leads to coupling of the vector controller from the plant, i.e. the induction motor. Consequences of such a coupling include the initiation of oscillations of the rotor flux and unsuitable switching of electromagnetic torque for the induction motor servo drive. Therefore, this paper describes a rotor resistance parameter compensating method for the induction motor. And the validity of the proposed design method is confirmed by simulation studies and experiment results.

1. Introduction

The performance requirements of many dynamic systems, such as NC machines, paper mill, space vehicles, and guided missiles, include optimization of the overall response to commands in order to ensure successful mission. One of the important modes of the optimum control is the time optimal control mode, which is also aferred to as the minimum control mode. The time optimal control scheme hes successfully applied to the separately excited dc motor drive systems[1, 2].

Most of the controlled electrical drives are at present dc-drives. The control of a dc machine is straight forward due to the decoupled orthogonal field and armature axis. However, the mechanical construction of these machine is complicated and the machine is expensive. In contrast, ac machines (squirrel cage type) have a simpler and robust

*正 會 員 : 서울大 大學院 電氣工學科 博士課程
**正 會 員 : 成均館大 工大 電氣工學科 助教授 · 工博
***正 會 員 : 서울大 工大 電氣工學科 教授
接受日字 : 1991年 6月 10日
1次修正 : 1991年 10月 23日

construction which permits high speed and reliable maintanance-free operation.

In the case of induction motor, however, the time optimal control scheme is rarely used because of its high order and nonlinear dynamics. That is very difficult to get the good transient characteristics, compared with dc motors, for the coupling effect between the flux and torque current. Introducing the vector control by which the flux and torque current is decoupled and controlled independently, these difficulties can be overcome. The induction motor with the vecotr control can have the transient performance nearly equal or even superior to that of the dc motor and it can be modeled with the second order[3].

The strategy of time optimal control for CSI fed induction motor servo system has been reported. But at low frequency region, CSI fed induction motor servo system cannot achieve good performance[4]-[7], [14].

Current control of voltage fed PWM inverter supplying induction motor can be achieved by means of hysteresis control. It give fast response and good accuracy. It can be implemented by minimum hardware and does not require knowledge of load parameters.

In this paper, the vector control system of the current controlled PWM inverter fed induction servo drive is proposed to obtain good dynamic response, which has superior control characteristic and can be implemented easily[8].

The performance of vector control by the slip frequency control method, however, depends heavily upon the accuracy of induction motor parameters. It has been know that changes in rotor resistance have a most dominant effect on control process.

In time optimal control problem, the performance index depends only on time. The control input $u(t)$ to minimize this performance index should be determined by solving Hamiltonian equation[9].

The time optimal position control scheme can be repeatedly taken from the initial state of a dynamic system to a desired one as fast as possible at the industrial drives. In this case, an induction machine parameters will very due to temperature, frequency, and saturation effects. In particular, the rotor resistance value changes dramatically with temperature and frequency. These changes affect the command values of the stator current components and slip speed.

There is a mismatch between the commanded variables and actual ones of the induction motor drive, and this situation leads to coupling of the vector controller from the plant, i.e. the induction motor. Consequences of such coupling include the initiation of oscillations of the rotor flux and unsuitable switching of electromagnetic torque of the induction motor servo drive[10], [11].

Previous work in this area, rotor parameter compensating methods for the induction motor have been developed[12]~[17].

The proposed control scheme applied to current controlled PWM inverter induction motor system. It is an indirect flux sensing method wherein the rotor flux is estimated from the stator current, voltage, and/or rotor speed. The time optimal position control will derive analytically and its validity is verified with the digital computer simulations and the experiments with the prototype of 5HP.

2. Influence of Parameter Variation on the Time Optimal Position Control of Indirect Vector Control Induction Motor

It is necessary for obtaining a high performance response that the amplitude, frequency, and phase of motor current be operated and controlled so that torque produced by motor will follow a torque command quickly and correctly. This control method is know as a vector control. Functional diagram of the inverter-fed induction motor drive system is shown in Fig. 1, along with corresponding current phase diagram.

A few key equations are listed here to explain the system under consideration and the compensation method which implements parameter adaptation[12].

The induction motor system of the synchronously rotating reference frame is as follows:

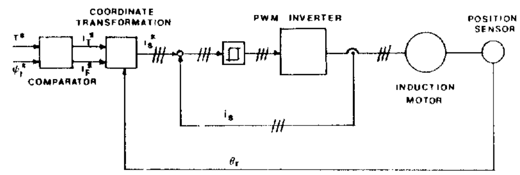

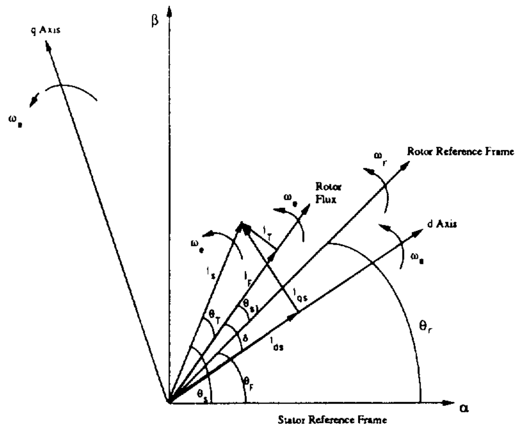

Fig. 1 Phasor diagram of the vector controlled induction motor drive.

$$\begin{bmatrix} V_{qs} \\ V_{ds} \\ 0 \\ 0 \end{bmatrix} = \begin{bmatrix} R_s+L_sp & \omega_e L_s & Mp & \omega_e M \\ -\omega_e L_s & R_s+L_sp & -\omega_e M & Mp \\ Mp & \omega_{s1} M & R_r+L_rp & \omega_{s1} L_r \\ -\omega_{s1} M & Mp & -\omega_{s1} L_r & R_r+L_rp \end{bmatrix} \begin{bmatrix} i_{qs} \\ i_{ds} \\ i_{qr} \\ i_{dr} \end{bmatrix} \tag{1}$$

The electromagnetic torque is

$$T=\frac{3P}{2}M(i_{qs}i_{dr}-i_{ds}i_{qr}) \tag{2}$$

where, P : number of pole pairs

The inputs to the vector controller are the torque and flux command. The d and q axis stator currents and slip frequency commands are generated using the following equations:

$$i_{ds}=\frac{\phi_r}{M} \tag{3}$$

$$i_{qs}=\omega_{s1} T_r i_{ds} \tag{4}$$

The magnitude of stator current is

$$I_s=\sqrt{i_{ds}^2+i_{qs}^2} \tag{5}$$

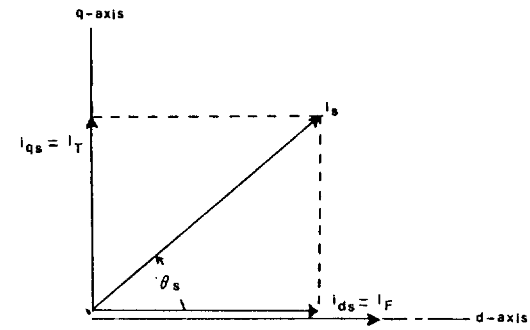

Fig. 2 Resolution of stator current along flux phasor.
(Case where decoupling is perfect $T_r=T_r^*$, ω_{s1}=suitable)

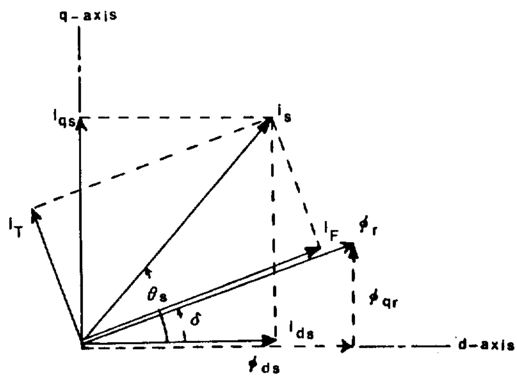

Fig. 3 Resolution of stator current along rotor flux phasor.
(Case where decoupling is not perfect $T_r < T_r^*$: too small)

i_{ds} is aligned along the rotor flux ϕ_r as shown Fig. 2

$$\omega_{s1}=\frac{1}{T_r}\frac{i_{qs}}{i_{ds}}\ ;\ \omega_e=\omega_{s1}+\omega_r \tag{6-a}$$

$$\omega^*_{s1}=\frac{1}{T_r^*}\frac{i_{qs}}{i_{ds}} \tag{6-b}$$

where, $T_r=L_r/R_r$

T_r^* : normal value of rotor time constant

If the angle between flux and d-axis is defined by δ in Eq. (7), this is related ΔT_r by the following equation

$$\sigma=\tan^{-1}\left[\frac{-\frac{\Delta T_r}{T_r}}{\frac{i_{ds}}{i_{qs}}+\left(1+\frac{\Delta T_r}{T_r}\right)\frac{i_{qs}}{i_{ds}}}\right] \tag{7}$$

where, $\Delta T_r = T_r - T_r^*$

If Eq. (6-a) is satisfied, d-axis is coincide with the flux axis. Fig. 2 shows the phasor diagram in this case. If the relation of Eq. (6-a) is not satisfied by the variation of T_r, the phasor diagram becomes as shown in Fig. 3. At this time the flux axis displaces from d-axis.

If the flux and d-axis are not coincide, the field current and torque current are expressed by the following equation.

$$i_F = i_{ds}\left(\cos\delta + \frac{i_{qs}}{i_{ds}}\sin\delta\right) \tag{8}$$

$$i_T = i_{qs}\left(\cos\delta + \frac{i_{ds}}{i_{qs}}\sin\delta\right) \tag{9}$$

$$\phi_r = Mi_F \tag{10}$$

In this case the developed torque is as following.

$$T = P\frac{M^2}{L_{r1}+L_r} i_{qs} i_{ds}\left[1-\sin\delta\cos\delta\left(\frac{i_{qs}}{i_{ds}}-\frac{i_{ds}}{i_{qs}}\right)\right] \tag{11}$$

And we must compensate the slip angular frequency by the $\Delta\omega_{s1}$, which is proportional to ΔT_r

$$\Delta\omega_{s1} = \omega_{s1} - \omega^*_{s1} = \left[\frac{1}{T_r} - \frac{1}{T_r^*}\right]\frac{i_{qs}}{i_{ds}} = \left[\frac{T_r^*}{T_r} - 1\right]\omega^*_{s1} \tag{12}$$

The flux vector is computed from stator terminal voltages and currents using the following equations:

$$\phi_r = \int (V_s - R_s i_s)dt - (L_s + L_{r1})i_s \tag{13}$$

The compensation signal D is the output of flux regulator and proportional to $\left(\frac{T_r^*}{T_r}-1\right)$.

$$D = \frac{T_r^*}{T_r} - 1 = \frac{\Delta R_r^*}{T_r}\ ;\ L_{r1}+L_r : \text{constant} \tag{14}$$

where, $\Delta R_r = R_r - R_r^*$

Consider the simplified open loop position control system in Fig. 4 whose dynamic are written by

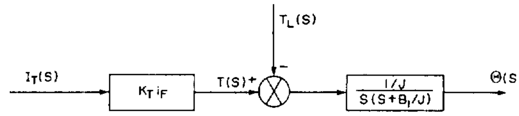

Fig. 4 Simplified second order system of induction motor.

$$d\theta/dt = \omega_r \tag{15}$$

$$d^2\theta/dt^2 = -\frac{B}{J}\frac{d\theta}{dt} + \frac{K_T i_T}{J} \tag{16}$$

$u(t) = i_T$ is used as control input in position system, assuming.

$$x_1(t) = \theta(t) - \theta_{ref},\ x_2(t) = \dot{x}_1(t) = +\omega_r$$

The state equation is obtained as follows:

$$\begin{bmatrix}\dot{x}_1(t)\\ \dot{x}_2(t)\end{bmatrix} = \begin{bmatrix}0 & 1\\ 0 & -a\end{bmatrix}\begin{bmatrix}x_1(t)\\ x_2(t)\end{bmatrix} + \begin{bmatrix}0\\ \frac{K_T}{J}\end{bmatrix}u(t) \tag{17}$$

where, a is B/J

The system is initially equilibrium $[x_2(0)=0]$ with a derivation from zero position $[x_1(0)=\theta(0) - \theta_{ref}]$. The final state must be in equilibrium with zero deviation:

$$[x_1(0)\ x_2(0)]^T = [\theta(0) - \theta_{ref}\ 0]^T \tag{18}$$

$$[x_1(t)\ x_2(T)]^T = [0\ 0]^T \tag{19}$$

The admissible control input is constrained by

$$|u(t)| \le i_{T\max} \tag{20}$$

The performance index for time optimal control is time T^*. Since we have

$$J_1 = \int_0^{T^*} dt = T^* \rightarrow \min. \tag{21}$$

Now the problem can be described as follows: determine a time optimal control $u(t)$ which minimizes the T^* from any initial state to the origin of the second order system with constraint on the control input[9].

3. Solution of Time Optimal Control Problem

Hamiltonian euqation of the system is

$$H = 1 + p_1(t)x_2(t) - ap_2(t)x_2(t) + \frac{K_T}{J}p_2(t)u(t) \tag{22}$$

thus the minimum principle indicates that the optimal control $u^*(t)$ must satisfy

$$p_2^*(t)u^*(t) \leq p_2^*(t)u(t) \quad (23)$$

And a is positive real number. The eigenvalues of this system equation (17) are 0 and $-a$; thus, since both eigenvalues are real and nonpositive, it has been proved that there must exist for the system on unique optimal control taking the system from any initial state to the origin and has as most $(n-1)$ switchings[7], [9]. From the minimum principle, we obtain

$$u^*(t)=\begin{bmatrix} -i_T \text{ for } p_2^*(t)>0 \\ +i_T \text{ for } p_2^*(t)<0 \end{bmatrix} = -\text{sgn}(p_2^*(t)) \quad (24)$$

It is obvious that the control $u(t)$ can switch at most 1 times and take piecewise constant sequence $(-i_T, +i_T)$ or $(+i_T, -i_T)$. We first determine the set of points from which the origin can be reached with $u(t)=-i_T$ (call this set V_1^+), and the set of points from which the origin can be reached with $u(t)=-i_T$ (call this set V_1^-). Define V_1 to be the set of all states from which the origin can be reached in positive time by applying the single constant control $u(t)=i_T$ or $u(t)=-i_T$. The solutions are

$$x_2(t)=\pm\frac{1}{a}(1-e^{-at}) \quad (25)$$

$$x_1(t)=\pm\frac{1}{a}t\pm\frac{1}{a^2}e^{-at}\mp\frac{1}{a^2} \quad (26)$$

To determine V_1^+, use the upper sign (which corresponds to $u(t)=i_T$), solve (25) for t, and substitute in (26) to obtain the relationship

$$x_1(t)=-\frac{1}{a^2}ln\left(-a\left[x_2(t)-\frac{1}{a}\right]\right)-\frac{1}{a}x_2(t) \quad (27)$$

The set of points in the x_1-x_2 plane for which this equation is satisfied is V_1^+. Similar reasoning yields as expression for V_1^-.

$$V_1=\left\{x_1(t), x_2(t) : x_1(t)=\frac{1}{a^2}ln\left(a\left[x_2(t)+\frac{1}{a}\right]\right)-\frac{1}{a}x_2(t)\right\} \quad (28)$$

Since Eq. (27) applies for $x_2(t)<0$ and Eq. (28) applies for $x_2(t)>0$, the expression for V_1 (the set of all points that are in either V_1^+ or V_1^-) is given by

$$V_1=\{x_1(t), x_2(t) : x_1(t)=\frac{x_2(t)}{|x_2(t)|}\frac{1}{a^2} ln\left(a\left[|x_2(t)|+\frac{1}{a}\right]\right)-\frac{1}{a}x_2(t)\} \quad (29)$$

Thus the switching function is then

$$S(x(t))=x_1(t)-\frac{x_2(t)}{|x_2(t)|}\frac{1}{a^2} ln\left(a\left[x_2(t)+\frac{1}{a}\right]\right)+\frac{1}{a}x_2(t) \quad (30)$$

So we have solved our problem to find the optimal trajectory from an arbitrary starting point. And contro law is expressed as follows :

$$u(t)=\begin{cases} -i_T, \text{ for } x(t) \text{ such that } S(x(t))>0 \\ +i_T, \text{ for } x(t) \text{ such that } S(x(t))<0 \\ -i_T, \text{ for } x(t) \text{ such that } S(x(t))=0 \text{ and } x_2(t)>0 \\ -i_T, \text{ for } x(t) \text{ such that } S(x(t))=0 \text{ and } x_2(t)<0 \\ 0, \text{ for } x_1(t)=x_2(t)=0 \end{cases} \quad (31)$$

An implementation of this optimal control law is shown in Fig. 7 ; the required hardware consists of a summing device, a sign changer, a nonlinear function generator, and ideal relay.

4. Hardware Implementation

The proposed control strategy are applied to the current controlled PWM inverter fed induction motor system as follows. The 16bit microprocessor-based control system has been developed in the laboratory, which is suitable for implementing different control strategy. The motor parameters are listed in appendix. The microcomputer has a keyboard with versatile command keys that will aid in developing and debugging software for the control system. The hardware configuration of experimental system is shown in Fig. 5.

There are two feedback signals, the position and the speed. The position data is obtained from 16bit up/down counter which counts the pulse from the pulse encoder. The speed measurement is based on

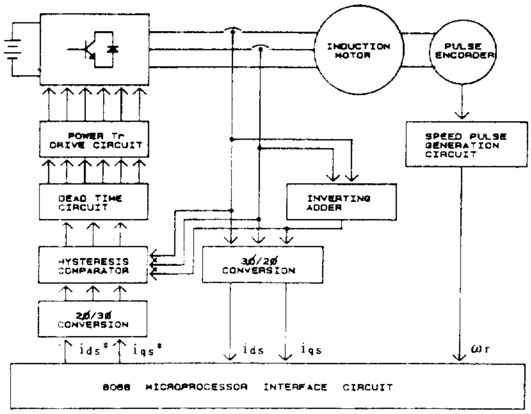

Fig. 5 Hardware configuration of experimental system.
(*indicates reference value)

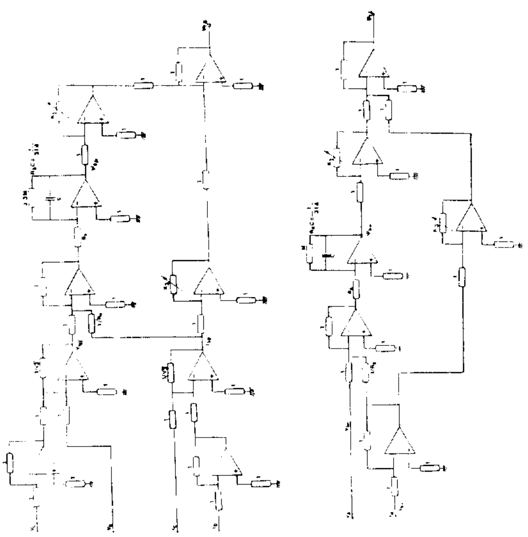

Fig. 6 Rotor flux computation circuit.

the M/T method. Considering the mechanical and electrical time constant, the position and speed control loop are executed every 10[msec] and current control loop every 2[msec], respectively. D/A converters are used to display the internal variables executed in the microprocessor.

The circuit diagram for the analog computation of rotor flux is shown in Fig. 6. The two's $\alpha-\beta$ as fluxes are computed from analog circuit and read into the microprocessor through $d-q$ axis trnsformation to obtain rotor flux[13].

5. Software Configuration for The time Optimal Position Control

Fig. 7 shows the overall block diagram of the time optimal control. As shown in fig. 6, time optimal controller is added to the conventional vector control loop of the current controlled PWM inverter fed induction motor. The field current i_F is usually kept constant to obtain high performance drive, and torque current i_T is determined by time optimal controller.

Switching function $S(x(t))$ is calculated by the position error, rotor speed and function generator and control input is determined to have through the ideal relay, the positive or negative maximum of torque current. Changes in temperature, current and slip frequency vary the machine parameters and hence indirectly influence both the steady state and dynamic operation of the drive system, ideally all parameters used in the vector controller should be modified as they change in the machine.

By reason of them, we set up a compensator in order to implement indirect vector control on high performance induction motor servo system.

By the time optimal controller, it takes the minimum time to reach the commanded position limiting the acceleration and deceleration rates

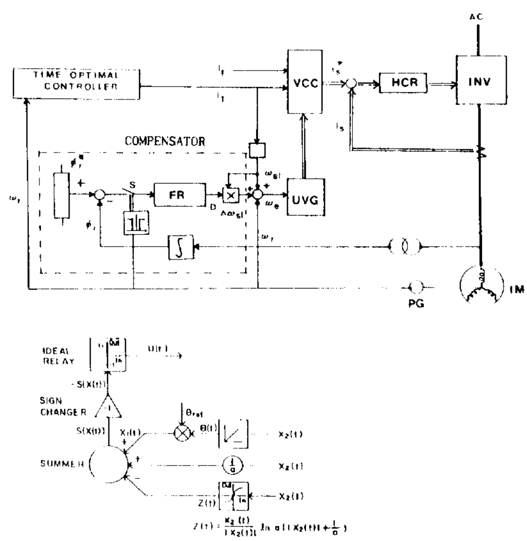

Fig. 7 The proposed compensating method block diagram.

and also rotor speed within the tolerable range. Therefore the speed pattern consists of the acceleration period, the constant speed period, and the deceleration period.

6. Simulation Results

To confirm the validity of the proposed control strategy, the digital simulation on system performance is executed. The system performance for the case of without and with compensation are compared to examine effectiveness of parameter adaptation. If the predicted flux deviates from the actual flux because of the variation rotor time constant, the axis of actual flux displaces from d-axis, and further the magnitude of the flux

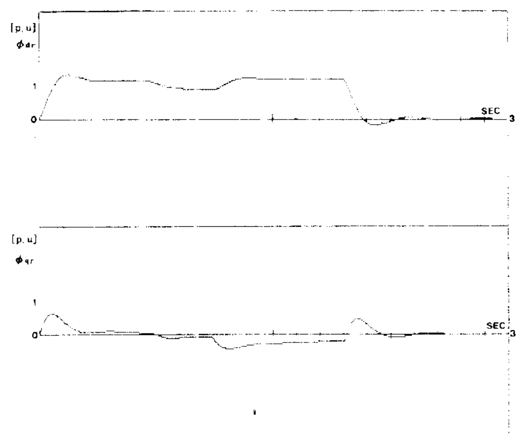

그림 8 The case of varied time constant and without compensation.
(a) d axis component of rotor flux
(b) q axis component of rotor flux

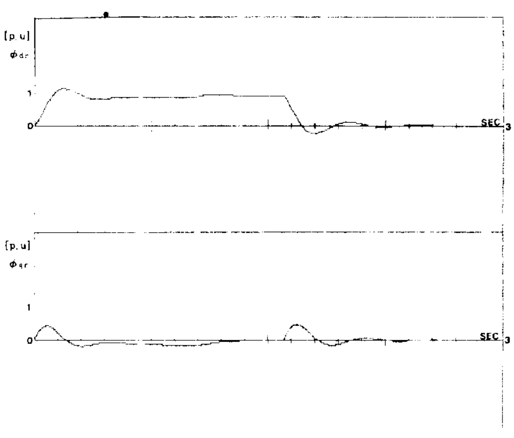

Fig. 9 The csae of varied time constant and with compensation.
(a) d axis component of rotor flux
(b) q axis component of rotor flux

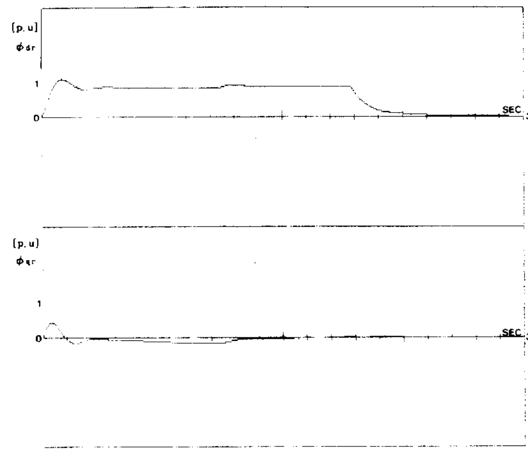

Fig. 10 The case of fixed time constant($\delta=0$).
(a) d axis component of rotor flux
(b) q axis component of rotor flux

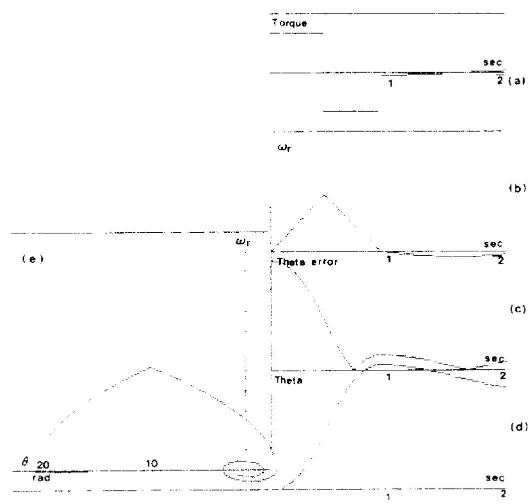

Fig. 11 The case of varied time constant and without compensation at $\theta_{ref}=20$[rad].
(a) torque reference, (b) speed
(c) position error, (d) position
(e) phase plane trajectory

deviates.

The d and q component of the rotor flux are shown in Fig. 8, Fig. 9 and Fig. 10.

In the simulation of Fig. 8~10, the d-q component of rotor flux is caculated by the equations

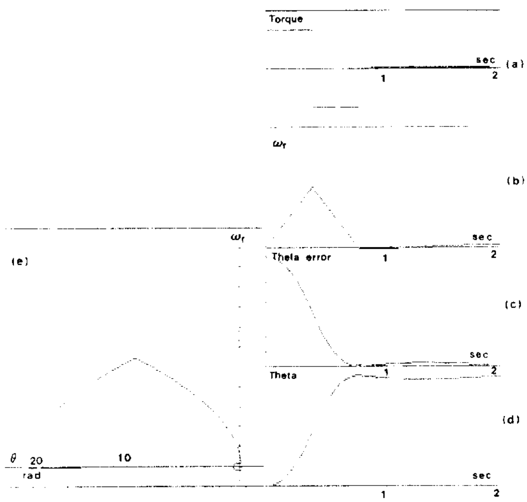

Fig. 12 The case of the fixed time constant at θ_{ref} =20[rad]
(a) torque reference, (b) speed
(c) position error, (d) position
(e) phase plane trajectory

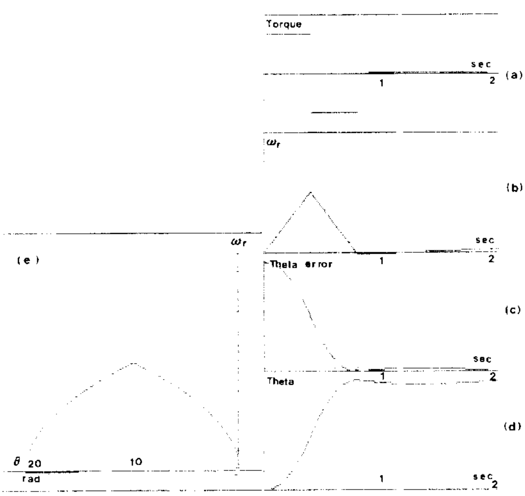

Fig. 13 The case of varied time constant and with compensation at θ_{ref}=20[rad].
(a) torque reference, (b) speed
(c) position error, (d) position
(e) phase plane trajectory

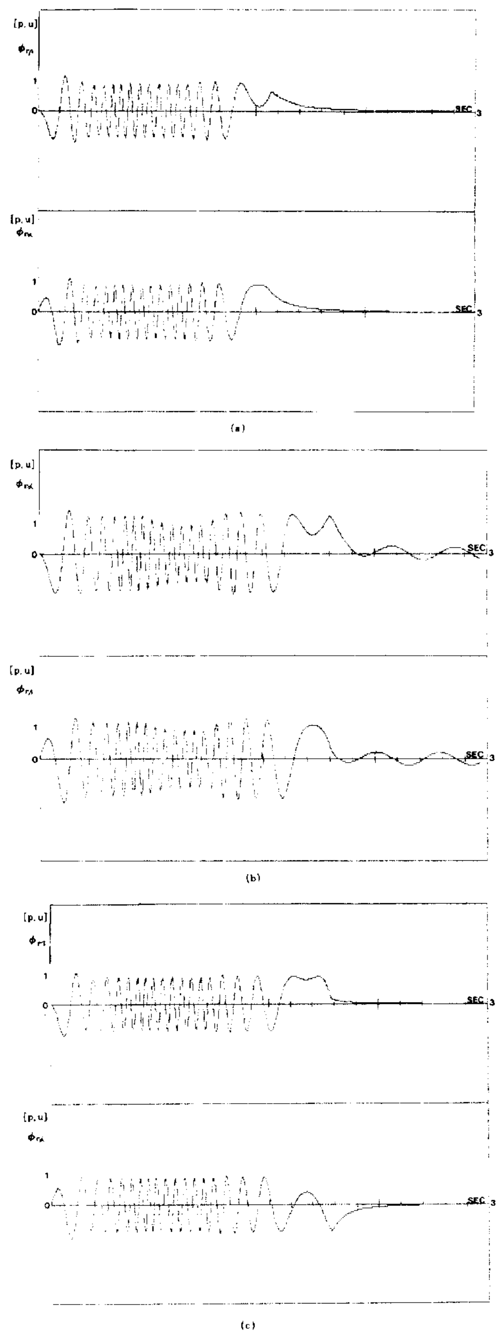

Fig. 14 Rotor flux waveform at the 100[rad].
(a) $\frac{T_r^*}{T_r}$=1(the case of fixed time constant)
(b) $\frac{T_r^*}{T_r}$=1.5(without compensation)
(c) $\frac{T_r^*}{T_r}$=1.5(with compensation)

[12].

In Fig. 8, since the T_r is varied without compensation, the flux are very different from command value. The influence of the variation of the rotor time constnat T_r is produced by the fact that the optimum value of the slip angular frequency indicated in Eq. (6-a) deviates from the slip angular frequecny set value determined by Eq. (6-b).

In Fig. 9 the T_r is varied with compensation, and in Fig. 10, the rotor flux are much more like with the command value, comparing with the case of Fig. 8.

Fig 8~10 shows d-q component of rotor flux at the 100[rad/sec] such as Fig. 14.

Fig. 11, Fig. 12 and Fig. 13 shows the response of the system in each figure, (a) is the torque reference, (b) is the speed, (c) is position error, (d) is position and (e) is phase-plane trajectory.

Fig. 11 is the case of the varied time constant without compensation. Fig. 12 is the case when compensation is not needed because the T_r is not varied. Fig. 13 is the case of the varied time constant with compensation. Fig. 13 shows the similar response with the case of Fig. 12, but in Fig. 11 the response is much deteriorated because of the variation of T_r. Fig. 14 shows the waveform of rotor flux on stationary the reference frame. In the case of (a), the rotor flux is not deviated from the normal value, but in the case of (b), it is deviated largely because of the varied rotor time constant. On the otherhand, in the case of (c), if compensation is made, it is as good as the case of (a).

Therefore the induction motor servo drive system is necessary to compensate the variation of control charateristic by correcting slip angular velocity.

7. Experimental Results

Fig. 15 shows the software flow-chart. Software is composed of key scanning program, conversion program, time optimal control loop program, display program, main program including the time optimal operation and speed & position measurement program. Experimental results are shown in Fig. 16~18.

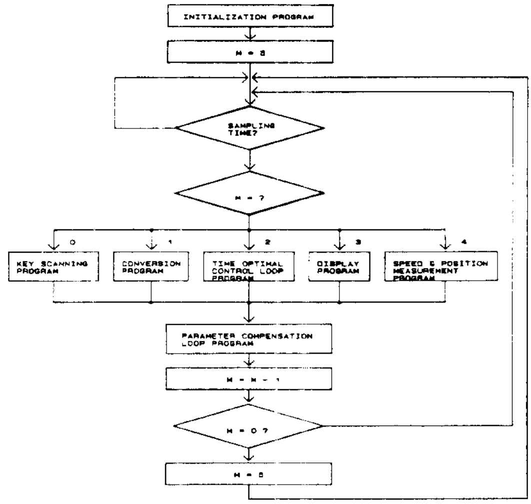

Fig. 15 Flow-chart of software.

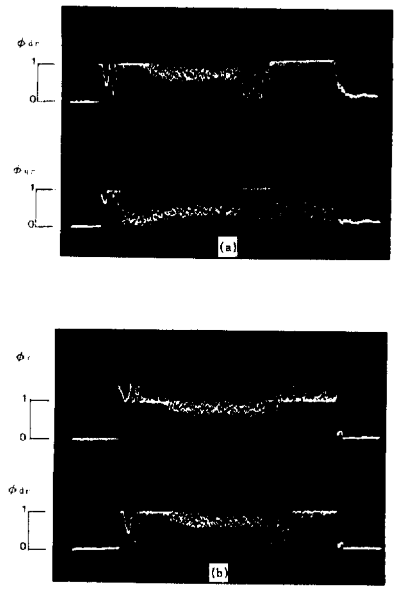

Fig. 16 Rotor flux waveform.

In the Fig. 18, the response of (b) is slower than (a) because of unsuitable switching.

8. Conclusion

On the basis of vector control, the time optimal position control scheme is conceived for three phase induction motor, which is driven by a cur-

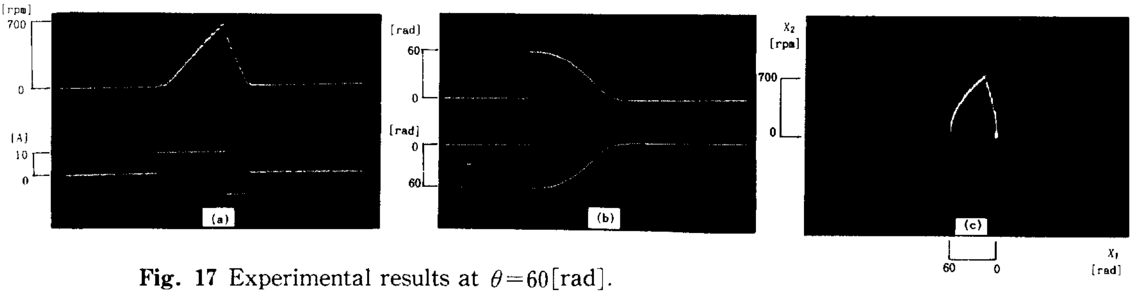

Fig. 17 Experimental results at $\theta=60$[rad].
(a) speed(upper), torque current(lower). (b) position error, position.
(c) phase plane portrait.

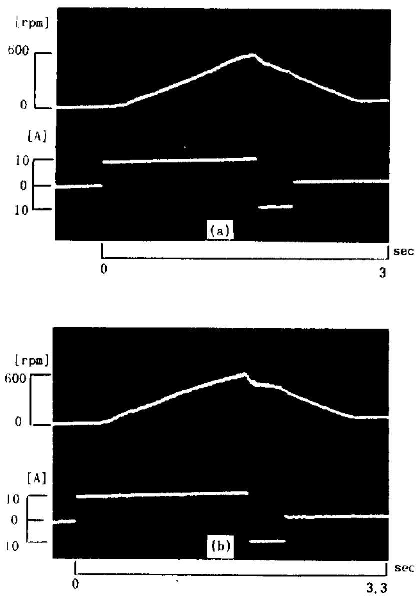

Fig. 18 The waveform of speed and torque current at $\theta_{ref}=100$[rad]
(a) $\frac{T_r^*}{T_r}=1.5$(with compensation)
(b) $\frac{T_r^*}{T_r}=1.5$(without compensation)

rent controlled PWM inverter with hysteresis controller. The following concluding remarks are confirmed.

1) The induction motor system with the vector control is regarded as the model equivalent to the DC motors, and then the Pontryagin's principle is applied to the system for the time optimal position control.
2) The vector control induction motor is modeled with the second order plant, and time optimal controller is constructed to derive control input from the Hamiltonian equation.
3) The performance of coupling control methods based on induction machine flux model can be influenced by mismatch between the parameters varies being used in the controller and the actual machine parameters. Therefore in this paper a parameter adaptation scheme has been proposed to compensate for the machine parameter variation.
4) Simulation and experiment are carried out to verify the feasibility of the proposed control strategy, and it is expected that the scheme of the time optimal control is useful to the high performance servo applications.

REFERENCES

[1] Cheng Bing, Yan Zhi-Tong and Lang Shi-Jun, "Time Optimal Position Controller for DC Motor Drive," IECON'84, pp. 604~610, 1984.

[2] B.H. Kwon, H.J. Park, J, Youn and T.Y. Ann, "Ditital Position Controller of PWM DC Motor for Improving Time Optimal Controller under the Inexact Load Parameter," IECON'86, pp. 253~258, 1986.

[3] F. Blaschke, "The Principle of Field Orientation as Applied to the New Transvector Closed-Loop Control System for Rotating Field Machines," Simens Review, Vol. 34, pp. 217~220, May 1971.

[4] M. Ishida, S. Somboon, S. Okuma and K. Iwata, "Time Optimal Control of Induction

Motor," IEEE Ind. Appl. Soc. Annu. Meeting, pp. 42~49, 1986.

[5] S. Sangwongwanich, M. Ishida, S. Okuma, Y. Uchikawa and K. Iwata, "Implementation of a Time-Optimal Signal Velocity Response Control Scheme of Field Oriented Induction Machines Considering Saturation of Flux," 19th Annual IEEE Power Electronics Specialist Conference, Proceeding PESC'88, pp. 1076~1083, 1988.

[6] Min H. par, Chung Y. won, "Microprocessor Based Time Optimal Position Control of a CSI Fed Induction Motor," Proceeding TENCON'87, IEEE REGION 10 CONFERENCE, pp. 1000~1005, 1987.

[7] Gi T. Kim, Kyung S. Kim, Min H. Park, Chung Y. Won and Doo, S. Ahn, "Time Optimal Control for Induction Motor Servo System," 19th Annual IEEE power Electronics Specialist Conference, Proceeding PESC'88, pp. 1053~1062, 1988.

[8] D.M. Brond and D.W. Novotny, "Current Control of VSI-PWM Inverters," IEEE Trans. Ind. Appl., Vol. IA-21, 1985.

[9] Donald E. Kirk, Optimal Control Theory An Introduction, Prentice-Hall, 1970.

[10] R. Krishnan and P. Pillay. "Parameter Sensitivity in Vector Controlled AC Motor Drives," in Conf. Record IEEE-IECON'87, pp. 212~218, 1987.

[11] R. Krishnan, Frank C. Doran, "Study of Parameter Sensitivity in High Performance Inverter-Fed Induction Motor Drive System," IEEE Trans. Ind. Appl., Vol. IA-23, No. 4, pp. 623~635, July/Aug., 1987.

[12] T. Okuyama, et al., "High performace Ac motor Speed Control System using GTO Converters," in Conf. Record IPEC'83, Tokyo, pp. 720~731.

[13] S. Sathiakuma, et al., "Microprocessor-Based Field-Oriented Control of a CSI Fed Induction Motor Drive," IEEE Trans. Indus. Electron., Vol. IE-33, No. 3, pp. 39~43, Feb. 1986.

[14] Park Min-Ho, Won Chung-Yuen, Kim Young-Real, Kim Tae-Hoon, and Kim Hack-Seoung, "A Study on Parameter Sensitivity in Vector Control AC Motor Drive," KIEE Summer Meeting Conference, pp. 616~621, July 1989.

[15] Park Min-Ho, Kim Young-Real, Won Chung-Yuen and KIm Tae-Hoon, "A Study on Parameter Compensation Scheme in Vector Controlled Induction Motor Drive," KIEE Autumn Meeting Conference, pp. 20~24, November 1989.

[16] Won Chung Yuen, et al., "High Performance Control Strategy of Current Controlled PWM Inverter fed Induction Motor Servo Drive System," 15th Annual Conference of IEEE Industrial Electronics Society, Proceeding IECON'89, pp. 89~98, 1989.

[17] Won Chung Yuen, et al., "Microprocessor-based Field Orientated Control of a Current Controlled PWM Inverter-fed Induction Motor Servo Drive," Proceedings of 1990 IPEC, pp. 37~48, 1990.

Appendix

Motor Rating

Rated Voltage	220	V
Rated Current	15	A
Power	5	HP
Speed	1735	r/min
Frequency	60	Hz

Motor is three-phase delta connected with four poles.

Motor Parameter

$R_s = 0.434\ \Omega$

$R_r = 0.356\ \Omega$

$L_s = 0.0463$ H

$L_r = 0.0557$ H

$M = 0.0546$ H

J $= 0.21$ Kg · m²

$B = 0.019$ kg · m²/sec

NOMENCLATURE

i_{ds}, i_{qs} Two-phase d, q axis motor stator current variables

i_F	Current of flux component
i_T	Current of torque component or output of ideal relay
$i_{T\max}$	Maximum allowable current of torque componet
ϕ_{ds}, ϕ_{qs}	d, q component of stator flux
ϕ_{dr}, ϕ_{qr}	d, q component of rotor flux
ϕ_r	Rotor flux
I_s	Stator current vector
I_s^*	Reference current vector
ω_e	Synchronous angular velocity
ω_r	Rotor angular velocity
ω_{sl}	Slip angular velocity
θ_s	Synchronous angle
θ_F	Field angle
θ_{sl}	Slip angle
θ_r	Rotor angle
δ	Arbitrary fixed angle
P	Number of pole pairs
M	Mutual inductance
L_{r1}	Rotor leakage reactance
L_s	Stator reactance
L_r	Rotor reactance
VCC	Vector control caculator
UVG	Unit vector generator
FR	Flux regulator
HCR	Hysteresis current controller
SC	Speed controller
K_t, K_T	Torque constant
B	Friction coefficient
J	Moment of inertia of motor
$S(x(t))$	Switching function
$z(t)$	Function generator

저 자 소 개

김광헌(金珖憲)

1960년 12월 27일생. 1983년 전남대 공대 제어계측공학과 졸업. 1986년 서울대 대학원 전기공학과 졸업(석사). 1988년 동 대학원 전기공학과 박사과정 수료.

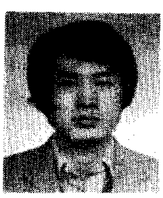

김영렬(金暎烈)

1958년 9월 5일생. 1982년 서울대 공대 전기공학과 졸업. 1982~87년 한국기계연구소 부설 기업 기술 지원센터 연구원. 1989년 서울대 대학원 전기공학과 졸업(석사). 현재 서울대 대학원 전기공학과 박사과정.

원충연(元忠淵)

1955년 5월 10일생. 1978년 성균관대 공대 전기공학과 졸업. 1980년 서울대 대학원 전기공학과 졸업(공박). 현재 성균관대 공대 전기공학과 조교수.

원종수(元鍾洙)

1928년 6월 27일생. 1952년 서울대 공대 전기공학과 졸업. 현재 서울대 공대 전기공학과 교수. 당학회 평의원.